Scaling properties of dynamical localization in monochromatically perturbed quantum maps: Standard map and Anderson map

Hiroaki S. Yamada

Yamada Physics Research Laboratory, Aoyama 5-7-14-205, Niigata 950-2002, Japan

Fumihiro Matsui

Department of Physics, College of Science and Engineering, Ritsumeikan University Noji-higashi 1-1-1, Kusatsu 525-8577, Japan

Kensuke S. Ikeda

College of Science and Engineering, Ritsumeikan University Noji-higashi 1-1-1, Kusatsu 525-8577, Japan



(Received 29 August 2017; published 16 January 2018)

Dynamical localization phenomena of monochromatically perturbed standard map (SM) and Anderson map (AM), which are both identified with a two-dimensional disordered system under suitable conditions, are investigated by the numerical wave-packet propagation. Some phenomenological formula of the dynamical localization length valid for wide range of control parameters are proposed for both SM and AM. For SM the formula completely agree with the experimental formula, and for AM the presence of a new regime of localization is confirmed. These formula can be derived by the self-consistent mean-field theory of Anderson localization on the basis of a new hypothesis for the cut-off length. Transient diffusion in the large limit of the localization length is also discussed.

DOI: 10.1103/PhysRevE.97.012210

I. INTRODUCTION

In one-dimensional quantum systems, strong localization phenomena have been observed due to large quantum interference effect when disorder exists in the system. A quite similar localization phenomenon occurs in classically chaotic dynamical systems which exhibit chaotic diffusion in the classical limit. A typical example of the former is one-dimensional disordered systems (1DDS) [1,2], and the latter one is the quantum standard map (SM) [3]. It has been shown that the localization of the wave packet can be delocalized by applying dynamical perturbation composed of a few number of coherent modes [4–11]. If the number of the modes is more than two, the delocalization takes place through a localizationdelocalization transition (LDT) accompanied by remarkable critical phenomena as the perturbation strength is increased. It has been explored in detail the transition process from the localized phase for mode number more than two.

In the previous paper [12], we also investigated quantum diffusion of an initially localized wave packet in the polychromatically perturbed Anderson map (AM), which is a time-discretized version of the Anderson model, in comparison with the SM driven by the same polychromatic perturbation. However, the nature of quantum diffusion exhibited by the monochromatically perturbed AM and SM, which has been supposed to be localized, have not still been well-investigated, except for early stage studies on SM [13].

Experimentally, Manai et al. observed the critical phenomenon of the LDT for Cesium atoms in an optical lattice [6], which is an experimental implementation of the perturbed SM, and the observed results were successfully interpreted as a three-dimensional LDT based on the equivalence between

SM and multi-dimensional disordered lattice by the so-called Maryland transform [14]. Their results are also interpreted by the self-consistent theory (SCT) of the weak localization in three-dimensional disordered system (3DDS) [4–11]. Further, they recently observed the localization phenomenon in the SM driven by coherent monochromatic perturbation [15]. This work is a very important experimental contribution in the sense that it first succeeded in realizing the two-dimensional disordered system (2DDS) as a monochromatically perturbed SM in the optical lattice. To confirm the presence of localization, very long time-scale data must be examined, which is very difficult in real experiment but is much easier in numerical simulation. After the early report suggesting the presence of localization [13], there has been no work of numerical simulation for the monochromatically perturbed SM.

The experimental results should be examined by reliable numerical simulation taking sufficiently long time steps, which will be done in the present paper. We note also that there have been several studies on the localization of the coupled SM, which can be identified with the 2DDS by the Maryland transform [16,17], but no definite quantitative results have been established, because long time-scale simulation of coupled rotors is much more difficult than the monochromatically

There are two main purposes in the present paper. One is to explore systematically the localization characteristics of the monochromatically perturbed SM with the numerical and theoretical methods. We focus our investigation on the quantum regime in which the coupling strength is smaller than a characteristic value decided by the Planck constant, and we reexamine the validity of the experimentally observed result of the Manai et al. in a wide parameter range of the

quantum regime. Our results are interpreted by the SCT of the localization based on a newly proposed hypothesis.

Another purpose is to report the characteristics of monotonically perturbed AM in comparison with the perturbed SM mentioned above, whose localization property has not been fully investigated. The AM is close to the original model of random lattice proposed by Anderson in a sense that randomness is explicitly included, and has its own physical origin quite different from the SM. Note that there have been some publications for numerical results of AM [18–20], and the presence of localization phenomenon for unperturbed and monochromatically perturbed AM was stressed, but the present paper is the first detailed quantitative exploration of the dynamical localization length and the scaling properties for the monochromatically perturbed AM. The parameter dependence of the localization length on the disorder strength and perturbation strength are given numerically, and it is theoretically interpreted based on the SCT of the localization.

Our main concern is whether or not the above-mentioned two models with quite different physical origin share common features of the dynamical localization phenomenon. The outline of the paper is as follows. In the next section, we introduce model systems, monochromatically perturbed SM and AM, examined in the present paper. The numerical results of scaling properties of the localization length in the perturbed SM and AM are given in Secs. III and IV, respectively, and some empirical formula representing the localization characteristic are proposed. In particular, the existence of two different regimes of the localization is confirmed for AM. In Sec. V, these formula are consistently derived by the SCT of Anderson localization for anisotropic 2DDS [21,22] by introducing some hypothesis for the characteristic length as a cut-off in the self-consistent equation. In addition, the relation between SM and AM is made clear by the Maryland transform [14]. In Sec. VI, we discuss the characteristics of diffusion for both models observed transiently on the way to the final localization. The existence of the semiclassical regime beyond the quantum regime is emphasized for SM. The last section is devoted to summary and discussion. In the appendices, we give some complementary numerical results and a simple derivation of the Maryland transform in Sec. V.

II. MODELS

The model Hamiltonian of the periodically kicked system driven by dynamical perturbation of with the amplitude ϵ and frequency ω_1 is

$$H(\hat{p},\hat{q},t) = T(\hat{p}) + V(\hat{q})\{1 + \epsilon \cos(\omega_1 t + \phi_0)\}\delta_t, \quad (1)$$

where the system is kicked by the impulsive force of period τ ,

$$\delta_t = \sum_{m=-\infty}^{\infty} \delta(t - m\tau) = \frac{1}{\tau} \sum_{m=-\infty}^{\infty} \cos\left(\frac{2\pi}{\tau}mt\right).$$
 (2)

and it frequency $2\pi/\tau$ is incommensurate with ω_1

Here $T(\hat{p})$ and $V(\hat{q})$ represent the kinetic and potential energies, respectively, and \hat{p} and \hat{q} being the momentum and positional operators, respectively. The evolution for the unit time interval $[s\tau,(s+1)\tau]$ is represented by the unitary

operator,

$$U(s,\phi_0) = e^{-iT(\hat{p})\tau/\hbar} e^{-iV(\hat{q})\{1+\epsilon\cos(\omega_1\tau s + \phi_0)\}/\hbar},$$
 (3)

which is "nonautonomus" depending explicitly upon the step $s \in \mathbb{Z}$.

Instead of Eq. (1), we introduce an autonomous representation: consider the periodically kicked system perturbed by the oscillator represented by the angle $\hat{\phi}$ and acton $\hat{J} = -i\hbar d/d\phi$ operators, which we call hereafter the "J-oscillator":

$$H_{\text{tot}}(\hat{p}, \hat{q}, \hat{J}, \hat{\phi}, t) = T(\hat{p}) + \omega_1 \hat{J} + V(\hat{q})(1 + \epsilon \cos \hat{\phi})\delta_t, (4)$$

where $\omega_1 \hat{J}$ means the harmonic oscillator like energy of the J-oscillator. Then the corresponding unitary evolution operator for the time interval $[0, s\tau]$ is expressed by Eq. (3) as

$$U_{\text{tot}}(\tau s) = \mathcal{T}e^{-i\int_{0}^{s} H_{\text{tot}}(s')ds'/\hbar}$$

$$= e^{-i\omega_{1}\hat{J}\tau s/\hbar}\mathcal{T}e^{-i\int_{0}^{s} dt' [T(\hat{p})\tau + V(\hat{q})(1+\epsilon\cos(\omega_{1}t'+\hat{\phi}))]/\hbar}$$

$$= e^{-i\omega_{1}\hat{J}\tau s/\hbar}U(s,\hat{\phi})U(s-1,\hat{\phi})...U(1,\hat{\phi}), \tag{5}$$

where \mathcal{T} is the time ordering operator. Let us take the action eigenstate $|J=0\rangle$ as the initial state of the J oscillator. It is represented by the Fourier sum over the angle eigenstates as $|J=0\rangle=\frac{1}{\sqrt{J}}\sum_{j}^{J}|\phi_{j}\rangle$, where $\phi_{j}=2\pi j/J$. Then, applying Eq. (3), the wave-packet propagation by U_{tot} from the state $|J=0\rangle\otimes|\Psi_{0}\rangle$, where $|\Psi_{0}\rangle$ is an initial state of the kicked oscillator, is achieved by applying the periodically perturbed evolution operator $U(t,\phi_{0})$ of Eq. (3) to the initial state $|\phi_{0}\rangle\otimes|\Psi_{0}\rangle$ and next summing over ϕ_{0} . Summation over ϕ_{0} can be replaced very well by the ensemble average over randomly chosen ϕ_{0} [23]. We can thus use the representation of Eq. (3) for the numerical wave-packet propagation. But in theoretical considerations we often return to the representation of Eq. (4).

In the present paper, we set $T(\hat{p}) = \hat{p}^2/2$, $V(\hat{q}) = K \cos \hat{q}$ for SM, and $T(\hat{p}) = 2 \cos(\hat{p}/\hbar) = (e^{\partial/\partial q} + e^{-\partial/\partial q})$ (hopping between nearest-neighbor sites), $V(\hat{q}) = W v(\hat{q}) = W \sum_n \delta(q - n)v_q |q\rangle\langle q|$ for AM, respectively, where on-site potential v_n takes random value uniformly distributed over the range [-1,1] and W denotes the disorder strength.

In the autonomous representation, the Heisenberg equation (classical equation) of motion describing the monochromatically perturbed SM is

$$p_{s+1} - p_s = K \sin q_s (1 + \epsilon \cos \phi_s),$$

$$q_{s+1} - q_s = p_{s+1} \tau,$$

$$J_{s+1} - J_s = K \epsilon \cos q_s \sin \phi_s,$$

$$\phi_{s+1} - \phi_s = \omega_1 \tau,$$
(6)

where the Heisenberg operator is defined by $X_s := U^{\dagger}(1,\phi)..U^{\dagger}(s,\phi)\hat{X}U(s,\phi)..U(1,\phi)$. The set of equations for the monochromatically perturbed AM can be also obtained formally by the same way, but we should note that they have no classical counterpart.

In the case of SM, a chaotic diffusive motion occurs in the p space according to the mapping rule Eq. (6) in the classical limit $\hbar \to 0$, but the diffusion is localized if $\epsilon = 0$ for finite \hbar . On the other hand, the AM has no classical counterpart, but in the continuous limit $\tau \to 0$ with keeping $W/\tau \sim O(1)$, it become the Anderson model with the Hamiltonian $T(\hat{p}) + \{1 + \epsilon \cos(\omega_1 t)\}V(\hat{q})$, which exhibits localization in the q space in the limit of $\epsilon = 0$. Although the space in which the

localization occurs is different in SM and AM, the mechanism is considered as the same [14].

We explain here the numerical wave-packet propagation based upon the nonautonomous unitary evolution operator Eq. (3), in which ϕ is taken as classical number. The localization phenomena take place in the momentum (p) space for SM and in the position (q) space for AM, respectively. The momentum space of SM and the position space of AM are spanned by the momentum or position eigenfunctions. We denote the eigenfunction by $|n\rangle$, where $n \in \mathbb{Z}$, and the momentum and position are given as $p = n\hbar$ for SM and q = n for AM. Further, the periodic boundary condition is imposed on the wave function $|\Psi\rangle$ as $\langle n+N|\Psi\rangle = \langle n|\Psi\rangle$ for momentum (SM) and position (AM) representations, and suppose that the integer value n is bounded as $-N/2 \leqslant n \leqslant N/2$ for a very large positive integer N.

Let the wave packet at the step t be

$$|\Psi_t\rangle = U(t,\phi_0)U((t-1),\phi_0)...U(1,\phi_0)|\Psi_0\rangle,$$
 (7)

starting with the localized state $|\Psi_0\rangle = |n_0\rangle$ in the momentum (SM) or in the position (AM) space. We monitor the time-dependent mean-square displacement (MSD), $m_2(t) = \langle \sum_{n=-\infty}^{\infty} (n-n_0)^2 | u(n,t) |^2 \rangle_{\Omega}$ for the propagating wave packet $u(n,t) = \langle n|\Psi_t\rangle$, where $\langle \dots \rangle_{\Omega}$ denotes the ensemble average over initial condition n_0 for SM and different random config-

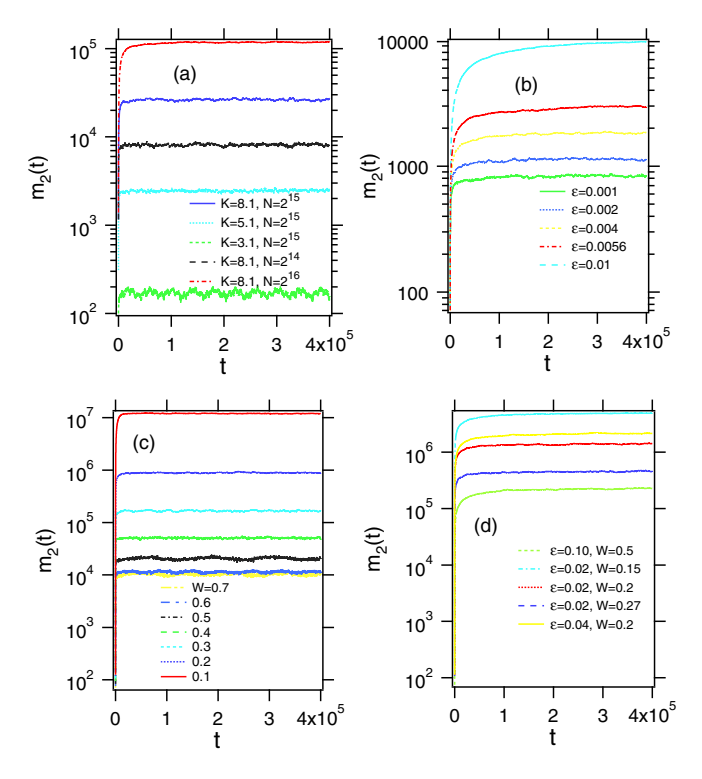


FIG. 1. The time-dependence of the MSD of SM and AM. (a) Unperturbed SM for K=3.1,5.1,8.1 with $\hbar=\frac{2\pi\,1248}{2^{15}}$, and for K=8.1 with $+\hbar=\frac{2\pi\,1248}{2^{14}},\frac{2\pi\,1248}{2^{16}}$. (b) Monochromatically perturbed SM for K=3.1 and $\hbar=0.12$ with $\epsilon=0.001\sim0.01$ from below. (c) Unperturbed AM with $W=0.1\sim0.7$ from top. (d) Monochromatically perturbed AM with some combinations of ϵ and W. Note that the horizontal axes are in logarithmic scale. The system and ensemble sizes are $N=2^{15}-2^{16}$ and 10-50, respectively, thorough this paper.

uration of v(n) for AM, respectively. In addition, the average over ϕ_0 should be taken, but the ϕ_0 dependence of the MSD is much weaker compared with the dependency upon n_0 (for SM) and sample of v(n) (for AM), and the averaging is ignored if unnecessary [24].

In this paper, we compute the localization length (LL) of the dynamical localization, $p_{\xi} = \sqrt{m_2(\infty)}$ for SM and $\xi = \sqrt{m_2(\infty)}$ for AM, after numerically calculating the MSD for long-time, where $m_2(\infty)$ is numerically saturated MSD. In fact, Fig. 1 shows the time-dependence of MSD for some unperturbed and perturbed cases in SM and AM. It is found that the growth of time-dependence is saturated and the LL becomes larger values as the perturbation strength becomes larger.

Note that it is difficult to get the accurate LL as the perturbation strength increases for cases with the larger K/\hbar in SM and smaller W in AM because of explosive increase of MSD. Then we also use the time-dependent diffusion coefficients to characterize the transient behavior before reaching the LL as will be discussed in Sec. VI.

III. LOCALIZATION PHENOMENA IN MONOCHROMATICALLY PERTURBED QUANTUM SM

In this section, we show the localization characteristics of the monochromatically perturbed SM with changing the three parameters K, \hbar , and ϵ in a wide range. We focus on the results of numerical experiments in the "quantum regime" where ϵ is smaller than a certain characteristic value dependent upon \hbar , which will be discussed later. On the other hand, it has been numerically and experimentally observed that, if \hbar is small enough, then classical diffusion of coupled SMs, which can be identified with 2DDS, is restored over a long time scale. Problems related to the classical diffusion will be discussed in Sec. VI.

As was already demonstrated in the experiments by Manai *et al.*, a remarkable feature of the SM with monochromatic perturbation is a definite exponential growth of the localization length with respect to the perturbation strength ϵ [15], namely,

$$p_{\xi} = D \exp\{\epsilon A\},\tag{8}$$

where the constants A, D are determined by K and \hbar . The experiment of Manai *et al.* was done for \hbar greater than unity, i.e., in a strong quantum regime.

Figure 2 shows ϵ dependence of the localization length p_{ξ} for some \hbar 's and K's. All the plots tell that Eq. (8) works quite well. Validity of Eq. (8) was confirmed for all values of K and \hbar we examined. The ϵ dependence has already been suggested in several papers [13,16,17]. In the following, we discuss the K dependence and the \hbar dependence of the coefficients A, D, by the intercept and the slope numerically determined by the semilog plot of Fig. 2. The details of the technical process for determining coefficients A and D in Eq. (8) are given in Appendix A.

As a result, we plot the coefficients A and D in Fig. 3 as a function of K/\hbar fixing \hbar at two significantly different values $\hbar = 0.56$ and 3.1 and changing K. The coefficients A and D are not only proportional to $(K/\hbar)^2$, but the two curves of A and of D overlap by extrapolation.

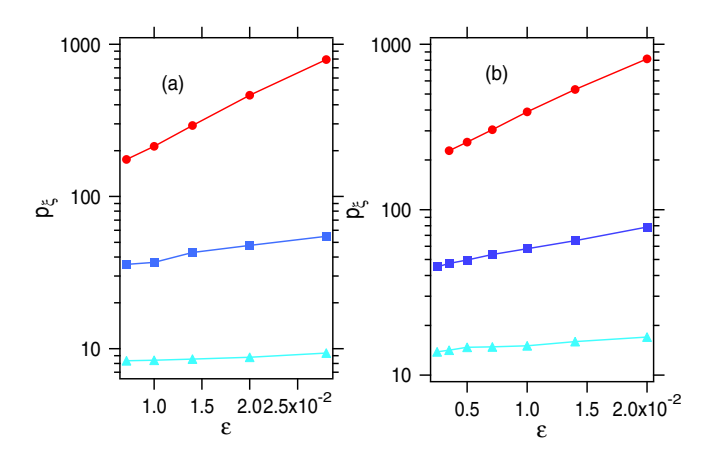


FIG. 2. Localization length p_ξ as a function of the relatively small perturbation strength ϵ in the quantum regime ($\epsilon=1\times 10^{-3}\sim 30\times 10^{-3}$). (a) K=3.1 for $\hbar=\frac{2\pi 435}{2^{12}},\frac{2\pi 435}{2^{13}},\frac{2\pi 435}{2^{14}}$ from below. (b) K=12.0 for $\frac{2\pi 1741}{2^{12}},\frac{2\pi 1741}{2^{13}},\frac{2\pi 1741}{2^{14}}$ from below. Note that the horizontal axes are in logarithmic scale.

Accordingly, the localization length of monochromatically perturbed SM is represented by

$$p_{\xi} \propto \left(\frac{K}{\hbar}\right)^2 \exp\left[\operatorname{const.}\epsilon \left(\frac{K}{\hbar}\right)^2\right]$$
 (9)

in the quantum regime. Note that in a limit of $\epsilon \to 0$, p_{ξ} becomes the localization length of the unperturbed SM $p_{\xi} \propto (\frac{K}{\hbar})^2$ first proposed by Casati *et al.* [3].

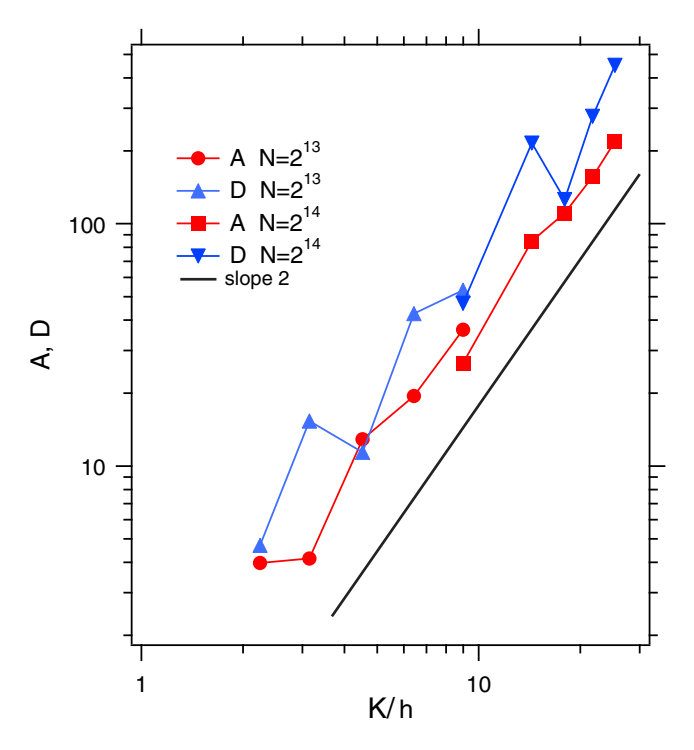


FIG. 3. (K/\hbar) dependencies of the coefficients A and D when varying the combination of K and \hbar variously. Note that the axes are in logarithmic scale. The heavy line shows a straight line with slope of 2 corresponding to the $(\hbar/K)^2$.

The results obtained above agree entirely with the experimental results of the Manai *et al.* They explained their results by applying self-consistent mean-field theory (SCT) to the monochromatically perturbed SM, and they obtained $A \propto (\frac{K}{\hbar})^2$, but $D \propto \frac{K}{\hbar}$, which is inconsistent with Eq. (9). A modified version of SCT of the localization naturally leading to the result Eq. (9) will be presented in Sec. VB. The modification is essential for the theoretical prediction of the localization length discussed in the next section.

IV. LOCALIZATION PHENOMENA IN MONOCHROMATICALLY PERTURBED AM

In this section, we show the numerical results for the localization characteristics of the monochromatically perturbed AM. The scaling properties of LL is explored by varying the disorder strength W and perturbation strength ϵ .

A. W dependence

It has been analytically found that in 1DDS the W dependence of the LL of eigenstates behaves like W^{-2} for weak disorder limit $W \ll 1$ by perturbation theory [25,26] and it decreases obeying $1/\log W$ in the strong disorder limit $W \gg 1$ [27,28]. Therefore, if the LL is almost the same as the dynamical localization length, we can expect the time-dependent spread of the initially localized wave packet is suppressed around the LL, and the W dependence of the saturated MSD behaves like $m_2(t) (= \xi_0^2) \sim W^{-4}$ in the weak disorder limit.

Based on these facts, we investigate the localization properties of the wave packet in the monochromatically perturbed AM. Figure 4 shows the W dependence of the LL in the system for various perturbation strength ϵ . First, let us focus on the unperturbed case ($\epsilon=0$) for which a typical situation of the localization in AM is expected to occur. It follows that the LL ξ_0 of the unperturbed case decreases like W^{-2} in the weak disorder regime as expected, but the decrease ceases around a certain value denoted by W^* , that is,

$$\xi_0 \simeq \begin{cases} c_0 W^{-2} & (W < W^*) \\ \xi_0^* & (W > W^*) \end{cases}$$
(10)

where c_0 is a constant and $\xi_0^* = \xi_0(W^*)$. The result is consistent with the perturbation theory only for the limit $W \ll 1$, as mentioned in Sec. II. Its reason is reconsidered with the Maryland transform in the next section, but very intuitively we can explain the presence of the characteristic value W^* above which the $\xi_0 \sim W^{-2}$ behavior changes to $\xi_0 \sim const$ by the periodic nature of the dynamical perturbation Eq. (2) in Sec. II. Equation (1) together with Eq. (2) allows us to interpret the original Hamiltonian of AM (set $\epsilon = 0$ for simplicity) as the Anderson model Hamiltonian $T(\hat{p}) + V(\hat{q})/\tau$ to which the dynamical perturbation $(2/\tau) \sum_{m=1}^{\infty} \cos(2\pi mt/\tau)$ of the period τ is added. The latter induces a transition between the localized eigenstates of the Anderson model if the typical energy width W of the localized states exceeds the minimal quantum unit $\hbar 2\pi/\tau$ of the periodic perturbation. Accordingly, it is expected that the δ function weakens the localization effect

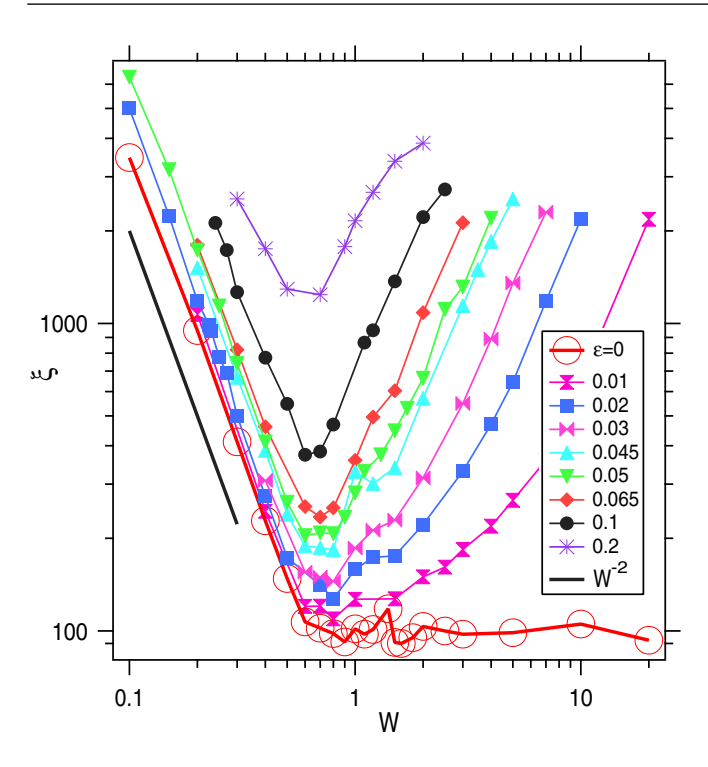


FIG. 4. Localization length of the monochromatically perturbed AM as a function of disorder strength W for various perturbation strength ϵ . The unperturbed case ($\epsilon = 0$) is denoted by a thick line with large circles. Note that the axes are in the logarithmic scale.

when W exceeds the characteristic value

$$W^* \simeq \frac{2\pi}{\tau}\hbar. \tag{11}$$

Taking $\hbar=1/8$, $\tau=1$, the above formula yields $W^*\sim0.8$, which is consistent with the characteristic value of Fig. 4, above which the monotonous decrease obeying the W^{-2} law ceases. Indeed, we have confirmed the change of the value W^* obeys Eq. (11) by varying the period τ .

The curves of the LL for various values of the perturbation strength ϵ is over-plotted in Fig. 4. For $W < W^*$, the W^{-2} -dependence is stably maintained even for $\epsilon \neq 0$, but the LL increases with increase in the perturbation strength ϵ at least in the weak perturbation limit $\epsilon \ll 1$. On the other hand, for $W > W^*$, the LL grows up as the disorder strength W increases if $\epsilon \neq 0$. In the next subsection, we look into the details of the ϵ dependence of the LL for the two regions, i.e., $W < W^*$ and $W > W^*$, to clarify their characteristics.

B. ϵ dependence

Figures 5(a) and 5(c) show the result of the ϵ dependence in the the monochromatically perturbed AM for $W < W^*$ and $W > W^*$, respectively. It is obvious that the LL grows exponentially as the perturbation strength ϵ increases in the both cases. Therefore, in the same way as the case of SM the LL can be expressed as

$$\xi \simeq D\exp\{A\epsilon\}.$$
 (12)

The coefficient D should be the LL at $\epsilon = 0$ and so $D = \xi_0$, whose characteristics are given as Eq. (10). The most

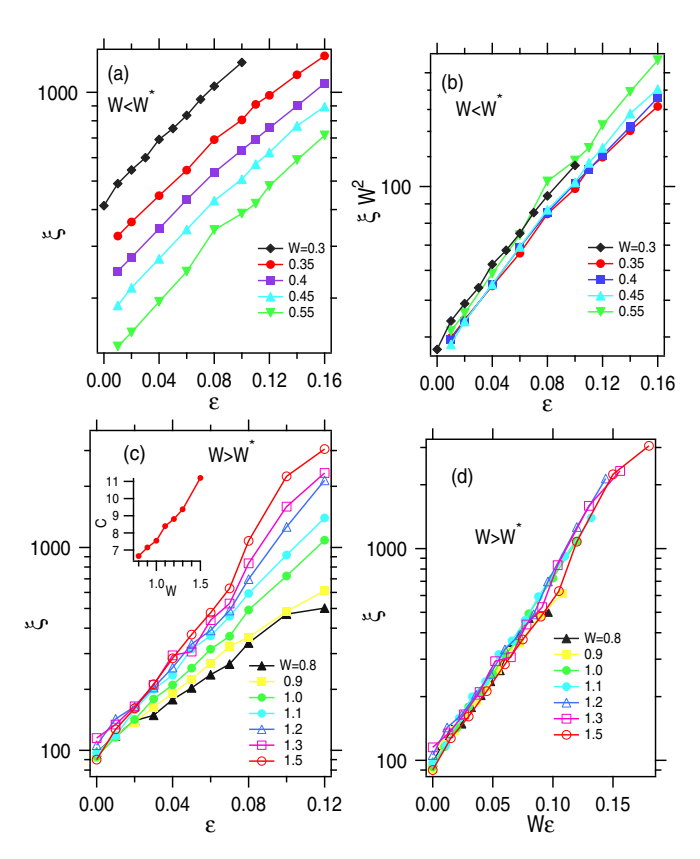


FIG. 5. Localization length of the monochromatically perturbed AM as a function of perturbation strength ϵ for (a) $W < W^*$, (c) $W > W^*$, where $W^* = 0.8$. (b) Plot of ξW^2 as a function of ϵ for $W < W^*$. (d) Plot of ξ as a function of ϵW for $W > W^*$. Note that the all the vertical axes are in the logarithmic scale. The inset in panel (c) shows the plot of the coefficient A as a function of W, which are estimated by linear fitting for data in the panel.

interesting point is the W dependence of the coefficient A in the two characteristic regions, $W < W^*$ and $W > W^*$. For $W < W^*$ the coefficient A is almost independent of W, and $\xi W^2 \propto \xi/\xi_0 = \xi/D$ as a function of ϵ overlaps each other as shown in Fig. 5(b). As a result, we can obtain the relation $\xi \sim c_0 W^{-2} \exp\{c_1 \epsilon\}$, where c_0 and c_1 are certain constants.

On the other hand, in the region $W > W^*$ peculiar to AM, there is a trend that the coefficient A increases with W as seen in Fig. 5(c). The inset in Fig. 5(c) shows the slope (coefficient A) of the data in the Fig. 5(c) determined by fitting in the range of $0.01 < \epsilon < 0.08$ using the method of least squares. The W dependence of the slope increases almost linearly. Indeed, all the plots of the LL as a function of $W\epsilon$ overlap as shown in Fig. 5(d) for $W\epsilon \ll 1$. The same scaling behaviours have been observed for the cases with different frequency ω_1 as given in Appendix B.

As a result, the LL ξ of the monochromatically perturbed AM can be summarized as follows:

$$\xi \simeq \begin{cases} c_0 W^{-2} \exp\{c_1 \epsilon\} & (W < W^*) \\ \xi_0^* \exp\{c_2 W \epsilon\} & (W > W^*) \end{cases}$$
(13)

where c_0, c_1, c_2 are numerical constants and ξ_0^* is the saturated LL of the unperturbed case.

The W dependence of the coefficient A is very different from those in SM, although the exponential growth with respect to ϵ is common.

Beyond W^* the transition between the localized states due to the dynamical perturbation play the role of stopping the decrease of LL as is exhibited by Eq. (10). Recalling that the dynamical part of perturbation potential in AM is given by $\epsilon W v(n) \cos(\omega_1 t)$, it is interesting to see the fact that the perturbation amplitude $W\epsilon$ does not influence the LL until W exceeds W^* , which means that the effect of dynamical perturbation fully works only after the transition channel opens. Interpretation of Eq. (13) by SCT of the localization will be presented in next section.

V. THEORETICAL EXPLANATION

In this section, we first confirm the relationship among SM, AM, and 2DDS by the Maryland transform [14]. Next, we give a theoretical explanation for the scaling properties obtained numerically in the last two sections is given based on the self-consistent mean-field theory (SCT) of the Anderson localization in 2DDS [22].

A. autonomous representation and Maryland transformation

We return to the two degrees of freedom unitary-evolution operator

$$\hat{U}_{\text{tot}} = e^{-i\omega_1 \hat{J}\tau/\hbar} e^{-iT(\hat{p})\tau/\hbar} e^{-iV(\hat{q})(1+\epsilon\cos\hat{\phi})/\hbar}, \qquad (14)$$

which takes the monochromatic dynamical perturbation into account by the J oscillator in an autonomous way. It can be written as

$$\hat{U}_{\text{tot}} = e^{-i\hat{A}}e^{-i\hat{B}}e^{-i\hat{C}},\tag{15}$$

where

$$e^{-i\hat{A}} = e^{-\frac{i}{\hbar}[T(\hat{p}) + \omega_1 \hat{J}]\tau}, \tag{16}$$

$$e^{-i\hat{B}} = e^{-\frac{i}{\hbar}\epsilon \hat{V}(q)\cos\phi\tau},\tag{17}$$

$$e^{-i\hat{C}} = e^{-\frac{i}{\hbar}V(\hat{q})\tau}. (18)$$

 $\tau = 1$ in this paper. We consider an eigenvalue equation,

$$\hat{U}_{\text{tot}}|u_1\rangle = e^{-i\gamma}|u_1\rangle,\tag{19}$$

where γ and $|u_1\rangle$ are the quasi-eigenvalue and quasi-eigenstate, respectively. This eigenvalue problem can be mapped into the tight-binding form by the Maryland transform, which provides with the foundation for applying the analysis developed for the 2DDS to our systems. This formulation further gives rise to some remarks about our approach.

For the SM, the eigenvalue equation we take the representation using eigenstate $|m\rangle(m\in\mathbb{Z})$ of momentum \hat{p} and the action eigenstate $|j\rangle(j\in\mathbb{Z})$ of the J-oscillator as $u_1(m,j)=(\langle m|\otimes\langle j|)|u_1\rangle$. Then by applying the Maryland transform, Eq. (19) is transformed into the eigenvalue equation of the following two-dimensional lattice system (tight-binding model) with aperiodic and singular on-site potential for newly defined eigenfunction $|u\rangle$ related to the original one $|u_1\rangle$ with

an appropriate transform shown in Appendix C:

$$\tan \left[\frac{\hbar^2 m^2/2 + j\omega_1 \hbar}{2\hbar} \tau - \frac{\gamma}{2}\right] u(m, j)$$

$$+ \sum_{m', j'} \langle m, j | \hat{t} | m', j' \rangle u(m', j') = 0, \tag{20}$$

where the transfer matrix element is

$$\langle m, j | \hat{t} | m', j' \rangle = \frac{1}{(2\pi)^2} \int_0^{2\pi} \int_0^{2\pi} dq d\phi e^{-i(m-m')q} e^{i(j-j')\phi}$$

$$\times \tan \left[\frac{K \cos q(1 + \epsilon \cos \phi)}{2\hbar} \tau \right]. \tag{21}$$

This is the Maryland transformed eigenvalue equation including the additional degree of freedom contributing as the monochromatic perturbation in the monochromatically perturbed SM. The details of the derivation is given in Appendix C. In particular, note that in the semiclassical limit $\hbar \to 0$ the potential term become singular. Indeed, under the condition $|K\tau/\hbar| > \pi$ the transfer matrix element becomes the Fourier coefficient of a function having poles on the real axis and the transfer matrix element does not decay as $|m-m'| \to \infty$ and so the analogy with the normal 2DDS is lost.

On the other hand, for the AM, we use the representation $u(n,j)(=(\langle n|\otimes\langle j|)|\overline{u}\rangle)$ based on the eigenstates $|q=n\rangle$ of the site operator \hat{n} and the eigenstates $|j\rangle$ of the operator \hat{J} , and the Maryland transformed eigenvalue equation becomes

$$\tan\left[\frac{Wv_n + j\omega_1\hbar}{2\hbar}\tau - \frac{\gamma}{2}\right]u(n,j) + \sum_{n',j'}\langle n,j|\hat{t}|n',j'\rangle u(n',j') = 0,$$
 (22)

where

$$\langle n, j | \hat{t} | n', j' \rangle = \langle n, j | i \frac{e^{-i\epsilon W v(\hat{q})\cos\phi\tau/\hbar} - e^{i2\cos(\hat{p}/\hbar)\tau/\hbar}}{e^{-i\epsilon W v(\hat{q})\cos\phi\tau/\hbar} + e^{i2\cos(\hat{p}/\hbar)\tau/\hbar}} | n', j' \rangle.$$
(23)

In the case of $\epsilon \neq 0$, the evaluation of matrix elements is not easy since the stochastic quantity v_n is contained in addition to both operators \hat{q} and \hat{p} .

If we take $\epsilon = 0$ as the simplest case of the hopping term in the transformed equation of AM, it becomes

$$\langle n, j | \hat{t} | n', j' \rangle = \frac{1}{2\pi} \int_0^{2\pi} dp e^{i(n-n')p} \tan \left[\frac{\cos(p/\hbar)}{\hbar} \tau \right], \tag{24}$$

where $p=2\pi\hbar k/N$. In the small τ limit the above equation results in an eigenvalue equation of the Anderson model with the nearest-neighboring hopping because $\tan(x) \simeq x$. On the other hand, as W increases such that $\tau W/2\hbar$ exceeds $\pi/2$, the range of the on-site potential of Eq. (22) covers the maximal range beyond which the distribution of the on-site potential do not change. This is an alternative explanation for the saturation of the localization length beyond W^* , which has been discussed in Sec. IV A.

Furthermore, from the Maryland transformed Eqs. (20) and (22), with $\epsilon = 0$ the relationship between AM and SM can also be roughly estimated. In the case of nearest-neighboring hopping for AM, the disorder strength increases with W/\hbar . On

the other hand, the hopping strength increases with increase of K/\hbar for $K/\hbar \ll 1$ in the case of SM. If the hopping strength is normalized to be unity, the disorder strength becomes proportional to \hbar/K . Accordingly, we can also see that the correspondence is roughly given as

$$\frac{W}{\hbar} \Leftrightarrow \frac{\hbar}{K}.\tag{25}$$

B. Interpretation of the scaling properties based on self-consistent theory of the localization

Using the self-consistent theory of the mean-field approximation for the localization in the anisotropic 2DDS, we interpret the scaling characteristics on the numerical results for SM obtained in Sec. III and AM in Sec. IV, respectively.

Let $D_{\mu}(\omega)$ be the dynamical diffusion constant in the μ direction ($\mu=1,2$). It is modified from the bare diffusion constant $D_{\mu}^{(0)}$ due to the destructive quantum interference induced by the backward scattering process of potential and is determined by the following self-consistent equation:

$$\frac{D_{\mu}(\omega)}{D_{\mu}^{(0)}} = 1 - \frac{1}{\pi \rho} \frac{D_{\mu}(\omega)}{D_{\mu}^{(0)}} \sum_{q_1, q_2} \frac{1}{-i\omega + \sum_{\nu=1}^2 D_{\nu}(\omega) q_{\nu}^2}.$$
 (26)

The second term in the right-hand side indicates the reduction by the quantum interference effect. (ρ is the density of states.) In the localized phase, the ω -dependent diffusion coefficient has a form $D_{\mu}(\omega) \propto -i\omega$ and is related to a scale of the length $\xi(\omega)$ in the infinite system as follows:

$$\xi_{\mu}(\omega)^{2} = D_{\mu}(\omega)/(-i\omega), \tag{27}$$

which indeed becomes the localization length $\xi(\omega=0)$ [or $p_{\xi}(\omega=0)$], in the limit of $\omega\to 0$. Here the summation over the wave number q_{μ} is done up to the upper cutoff decided by the inverse of the characteristics length ℓ_{μ} 's, which are important parameters discussed below in detail. Then, Eq. (26) in the μ direction is rewritten by an integral form,

$$\frac{\xi_{\mu}(\omega)^{2}}{\ell_{\mu}^{2}}(-i\omega t_{\mu})$$

$$= 1 - \frac{\xi_{\mu}(\omega)^{2}t_{\mu}}{\ell_{\mu}^{2}} \frac{1}{\xi_{1}(\omega)\xi_{2}(\omega)} \Xi \left[\frac{\xi_{1}(\omega)}{\ell_{1}}, \frac{\xi_{2}(\omega)}{\ell_{2}}\right], (28)$$

where $t_{\mu} = \ell_{\mu}^2/D_{\mu}^{(0)}$ means the localization time, and

$$\Xi \left[\frac{\xi_1(\omega)}{\ell_1}, \frac{\xi_2(\omega)}{\ell_2} \right] \\
= \tilde{c} \int_0^{\xi_1(\omega)/\ell_1} \int_0^{\xi_2(\omega)/\ell_2} dQ_1 dQ_2 \frac{1}{1 + Q_1^2 + Q_2^2}, (29)$$

where \tilde{c} is an appropriate numerical factor of O(1). Here, the characteristic length ℓ_{μ} of the integration range is usually taken as the mean free path, but in this paper we will propose different characteristic length as shown below.

Taking the case of SM as an example, we show the difference of the length proposed in this paper (maximum distance) from the ordinary length (minimum distance) as the characteristic length ℓ_{μ} . Let the kicked system with the characteristic length ℓ_{1} be the main system and the J oscillator with the characteristic length ℓ_{2} the subsystem. The ordinary selection for ℓ_{μ} is the minimum distance given as the hopping

length $p(s + 1) - p(s) = K \sin q_s$ for a single-step evolution from Eq. (6). The mean-square values are

$$(\ell_1 \hbar)^2 = K^2 \langle \sin^2 q_s \rangle = K^2 / 2,$$
 (30)

$$(\ell_2 \hbar)^2 = K^2 \epsilon^2 \langle \cos^2 q_s \rangle \sin^2 \phi_s = K^2 \epsilon^2 / 4. \tag{31}$$

Here, $\langle ... \rangle$ indicates the quantum mechanical average with respect to the initial state. These correspond to the so-called mean free path. Another candidate is the maximum distance reachable in an infinite time scale represented by the total hopping length $p(\infty) - p(0) = \lim_{s \to \infty} K \sum_{s' < s} \sin q_{s'}$. Now we are considering the weak perturbation limit of ϵ in which the kicked system is decoupled from the subsystem and maintains the diffusive motion as $m_2(s) = \langle (p_s - p_0)^2 \rangle = D_{cl}s$, where D_{cl} is the classical diffusion constant, until the localization time which should coincides with the number of states in the maximum length, i.e., ℓ_1 of the main system. (This corresponds to the so-called Heisenberg time, and precisely a numerical factor must be multiplied, but we ignore it.)

On the other hand, the J oscillator (the color degrees of freedom) also exhibits a passive diffusive motion up to

$$t_2 = t_1 = \ell_1, \tag{32}$$

being driven by the same force as the main system [see Eq. (6)]. From Eq. (6) the MSDs are expressed:

$$\lim_{s \to \infty} \langle (p_s - p_0)^2 \rangle = \lim_{T \to \infty} \sum_{s \le T} D_{1s}, \tag{33}$$

$$\lim_{s \to \infty} \langle (J_s - J_0)^2 \rangle = \lim_{T \to \infty} \sum_{s \le T} D_{2s}, \tag{34}$$

where the time-dependent diffusion constants D_{1s} and D_{2s} are defined by

$$D_{1s} = K^{2} [\langle \sin^{2} q_{s} \rangle + \operatorname{Re} \sum_{s' < s} \langle \sin q_{s'} \sin q_{s} \rangle]$$
 (35)

$$D_{2s} = K^2 \epsilon^2 \left[\langle \cos^2 q_s \rangle \sin^2 \phi_s \right]$$

$$+\operatorname{Re}\sum_{s'$$

As the maximum diffusion lengths, ℓ_1 and ℓ_2 , are proposed,

$$\ell_1^2 \hbar^2 = \lim_{s \to \infty} \langle (p_s - p_0)^2 \rangle, \tag{37}$$

$$\ell_2^2 \hbar^2 = \lim_{s \to \infty} \langle (J_s - J_0)^2 \rangle. \tag{38}$$

The time-dependent diffusion constants are a given as $D_{1s} = D_1^{(0)}\hbar^2 = D_{\rm cl}$ and $D_{2s} \equiv D_2^{(0)}\hbar^2 \sim D_{\rm cl}\epsilon^2/2$ until $t_1 = t_2 = \ell_1$, but both collapse to zero beyond it. Then Eqs. (33)–(37) lead to

$$\ell_1^2 = D_1^{(0)} \ell_1, \tag{39}$$

$$\ell_2^2 = D_2^{(0)} \ell_1. \tag{40}$$

This is a general relation applicable to the case of AM as will be used later. If we suppose the Markovian limit that the autocorrelation function of the force term coming from

the main system is given by $\langle \cos q_s \cos q_{s'} \rangle = \langle \sin q_s \sin q_{s'} \rangle = \delta_{s,s'}/2$, then $D_1^{(0)} = D_{\rm cl}/\hbar^2 = K^2/2\hbar^2$, $D_2^{(0)} = \epsilon^2 D_1^{(0)}/2$, and $\ell_{1,2}$ is given as

$$\ell_1 = D_1^{(0)} = \frac{D_{\text{cl}}}{\hbar^2},$$

$$\ell_2 = \frac{\epsilon}{\sqrt{2}} D_1^{(0)}.$$
(41)

As the fundamental distance ℓ_1 , ℓ_2 , we use these "maximal distance" rather than the "minimal distance" taken by Manai *et al.* [15]. We further remark that one can easily check the one-dimensional version of Eq. (28) can give the localization length of the standard map $\frac{D_{cl}}{\hbar^2}$ only by assuming $\ell_1 = D_1^{(0)} = \frac{D_{cl}}{\frac{1}{2}}$.

Under the above setting, Eq. (28) tells that the factor $\frac{\xi_{\mu}(\omega)^2}{\ell_{\mu}^2}t_{\mu}$ is independent of μ , which means that

$$\frac{\xi_1(\omega)}{\ell_1} = \frac{\xi_2(\omega)}{\ell_2},\tag{42}$$

because $t_{\mu}=t_1$ from Eq. (32). Carrying out the integral in the right-hand side of Eq. (28) for $\mu=1$, using the above relation, one has

$$\frac{\xi_1(\omega)^2}{\ell_1^2}(-i\omega\ell_1) = 1 - \frac{\tilde{c}}{\ell_2}\log\left[1 + \frac{\xi_1(\omega)^2}{\ell_1^2}\right]. \tag{43}$$

Taking a limit $\omega \to 0$ and organizing the expressions, the localization length $\xi_1(0)$ becomes

$$\xi_1(\omega = 0) \sim \ell_1 e^{\ell_2/2\tilde{c}},\tag{44}$$

where $\ell_1 = \frac{D_{\rm cl}}{\hbar^2} = \frac{K^2}{2\hbar^2}$ and $\ell_2 = \frac{\epsilon D_{\rm cl}}{\sqrt{2}\hbar^2} = \epsilon \frac{K^2}{2^{3/2}\hbar^2}$ are two selected characteristic lengths, and \tilde{c} is a suitable constant. This corresponds to the localization length in SM under the monochromatic perturbation in the previous sections. We remark that in the case of typical isotropic 2DDS the characteristic length $\ell_1 = \ell_2 (=\ell)$ can be identified with the mean free path $\ell_{\rm mfp}$ and Eq. (44) yields the well-known result $\xi_{\rm 2dds} \sim \ell_{\rm mfp} e^{\pi \ell_{\rm mfp}/2}$.

We can straightforwardly apply the above analysis to the perturbed AM. In a similar way as in the case of SM, the diffusion length of the J oscillator is obtained by replacing the term $K\epsilon \cos q_s \sin \phi_s$ in Eq. (6) coming from the interaction potential $K\epsilon \cos q_s \cos \phi_s$ by the term $W\epsilon v(q_s) \sin \phi_s$ in the interaction potential of the AM as

$$\ell_2^2\hbar^2 \sim W^2\epsilon^2 \sum_{s,s'} \langle v(q_s)v(q_{s'})\rangle \langle \sin\phi_s \sin\phi_{s'} \rangle.$$
 (45)

Since the diffusion time of the kicked system is given by ℓ_1 ,

$$\ell_2^2 \hbar^2 \sim W^2 \epsilon^2 \ell_1 / 2. \tag{46}$$

Accordingly, in the case of AM

$$\ell_1 \simeq \begin{cases} 1/W^2 & (W < W^*) \\ 1/W^{*2} & (W > W^*) \end{cases} \tag{47}$$

Therefore,

$$\ell_2 \sim \epsilon \sqrt{W^2 \ell_1 / 2} \simeq \begin{cases} \epsilon / \sqrt{2} & (W < W^*) \\ \epsilon W / \sqrt{2} & (W > W^*) \end{cases}$$
 (48)

It follows that when these are used for Eq. (44), results are consistent with that obtained by the numerical calculation in the previous sections.

In the SM, it also means that what Manai *et al.* used to explain the experimental results could be derived directly from the theoretical considerations by our selection for the characteristic lengths as the cutoff of the integral of SCT of the localization. Our hypothesis Eq. (37) is more vital in SM dynamically perturbed by more than two colors, in which a localization-delocalization transition occurs [11]. Indeed, it predicts precise parameter dependence of the critical value of ϵ numerically observed [12].

VI. DIFFUSION CHARACTERISTICS

Up to the previous section, we investigated localization characteristics in a relatively small perturbation regime in which the LL can be decided numerically. The exponential growing rate of the localization length is enhanced by decreasing \hbar or by increasing W for SM and AM, respectively. It is quite interesting to see the transient behavior on the way to the final localization in the large limit of the exponentially enhanced LL. In the case of AM, the region $W > W^*$ is focused on because it is an essentially new region peculiar to the quantum map in which the quantum hopping is assisted by the kick perturbation. On the other hand, in the case of SM the limit $\hbar \to 0$ is of interest because it is the semiclassical limit in which the LL is much enhanced, and classical chaotic diffusion may be observed at least in the transient process, as has been first examined in coupled SM [29].

Figures 6(a) and 6(b) show the time-dependence of the MSD obtained for SM and AM by increasing the perturbation strength ϵ , where \hbar is fixed at a sufficiently small value for SM, and W is fixed to a large value such that $W \gg W^*$ for AM. It becomes localized if ϵ is small, but as ϵ is increased larger, a diffusive behavior emerges over a long time scale, which is apparently different from the monotonically localizing behavior typically seen in the Fig. 1 in Sec. II.

To observe the diffusive behavior qualitatively the timedependent diffusion coefficient defined by

$$D(t) = \frac{d\overline{m}_2(t)}{dt} \tag{49}$$

is convenient, where $\overline{m}_2(t)$ indicates a smoothed curve over a sufficiently long section of time including t. Figures 6(c) and 6(d) show the time-dependence of D(t) for the SM and AM, respectively. The time-dependent diffusion coefficient decreases with time being accompanied with fluctuation, but for sufficiently large ϵ the decrease of D(t) is so slow that its variation is detectable only in the logarithmic time scale. In the early stage it seems to decreases linearly in logarithmic time scale. We remark that in the case of SM, D(t) agrees with the classical diffusion coefficient D_{cl} in the very initial stage, reflecting the quantum-classical correspondence within the Ehrenfest time.

Next we characterize the ϵ dependence of the timedependent diffusion coefficient D(t). Consider the time evolution up to t = T. As is shown in Fig. 6 D(t) takes the minimum value at t = T, and D(T) = 0 means that the wave packet have localized until t = T. We are concerned with D(t) after

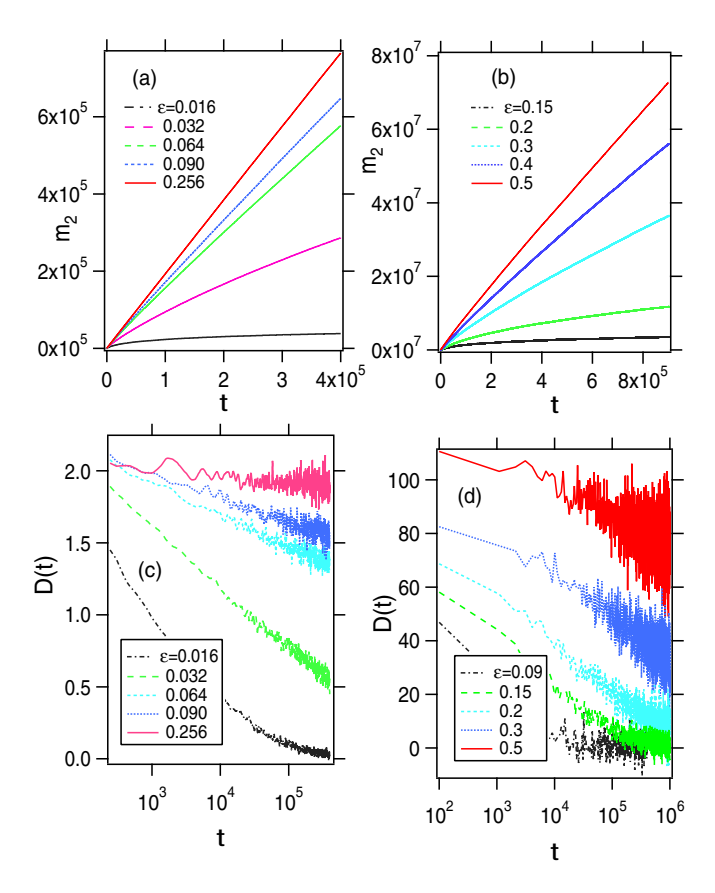


FIG. 6. The time dependence of the MSD and the diffusion coefficient D(t) for relatively large perturbation strength. (a) Monochromatically perturbed SM for K=3.1 with $\epsilon=0.016,0.032,0.064,0.09,0.256$ from below. (b) Monochromatically perturbed AM for W=1.0 with $\epsilon=0.15,0.2,0.3,0.4,0.5$ from below. (c, d) The D(t) of the SM and the AM, respectively. Note that the horizontal axes of the D(t) are in logarithmic scale.

a very long time evolution, but we cannot now specify the scale of T on which the dynamics of localization process is characterized. At present, we tentatively take the time scale T as long as our numerical run time allows, and we represent the minimum value D(T). T is fixed at $5 \times 10^5 - 10^6$ steps. The results are plotted as the function of the perturbation strength ϵ for three values of W (AM) and \hbar (SM) in Figs. 7(a) and 8(a), respectively. For the SM we also plot D(0), which is the maximum value of D(t) and mimics the classical diffusion constant D_{cl} , in order to show explicitly the range scanned by D(t) in the time interval $0 \le t \le T$. We plot also the classical diffusion coefficient D_{cl} as a function of ϵ . It follows that both in SM and AM the D(T) gradually rise with ϵ , and later it increases rapidly.

In the AM, the D(T) curve as a function of ϵ shifts upward with W, which is consistent with the dependence of LL on ϵ and W as discussed in the Sec. IV. In fact, taking the parameter $W\epsilon$ instead of ϵ the curves of diffusion coefficient D(T) in Fig. 7(a) are all well-overlapped, as shown in Fig. 7(b) if ϵW is not too large. Recalling the result of the previous Sec. IV that the single parameter $W\epsilon$ controls the LL, it is quite natural that the diffusion coefficients are also decided only by the combined parameter $W\epsilon$.

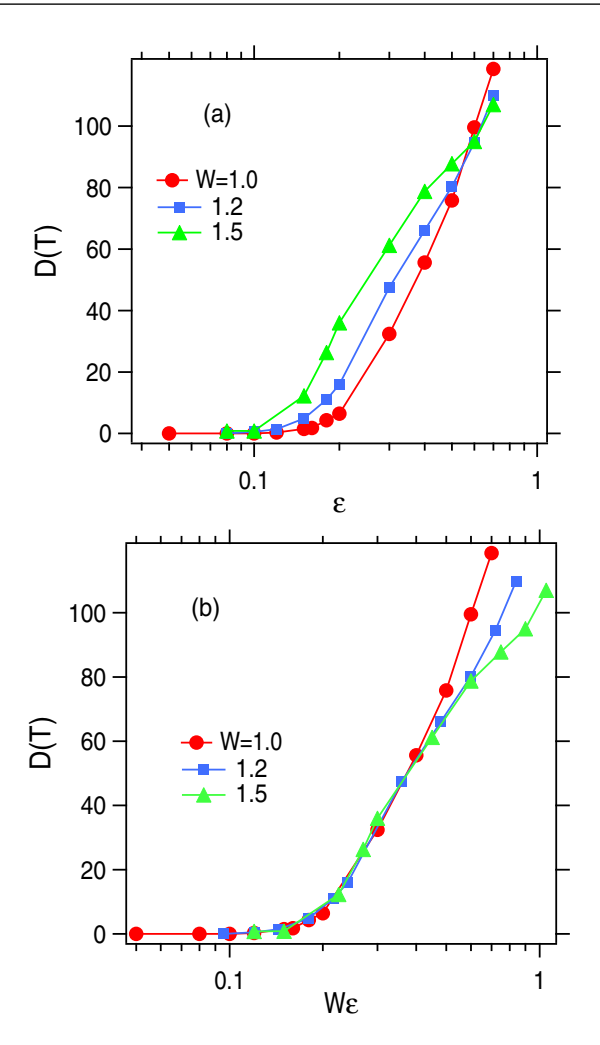


FIG. 7. (a) The time-dependent diffusion coefficient D(T) at $T=1\times 10^6$ as a function of ϵ in the monochromatically perturbed AM with W=1.0,1.2,1.5. (b) The D(T) as a function of $W\epsilon$. Note that the horizontal axes are in logarithmic scale.

Finally we discuss the very important feature of SM which is not seen in AM. It is the existence of the semiclassical regime which emerges for small \hbar , as was shown in coupled SM [29]. As mentioned above, D(0) mimics the classical diffusion coefficient, however, D(t) decreases as is shown in Fig. 6(c), and the decaying rate in $\log t$ scale decreases with ϵ , and there exists a characteristic value ϵ_c beyond which the decay becomes extremely small and so $D(T) \sim D(0) \sim D_{\rm cl}$. Indeed, Fig. 8(a) exhibits that with increase in ϵ , D(T) increases rapidly, and beyond a certain $\epsilon = \epsilon_c$ it forms a plateau on which D(T) keeps almost constant level. On the plateau the difference $D(T) - D(0)(\sim D_{cl})$ is small, and D(T) approaches closer to $D_{\rm cl}$ as $\hbar \to 0$. Thus we call the plateau as the "classical plateau" of the time-dependent diffusion coefficient. With further increase of ϵ , the classical diffusion rate is enhanced and D(T) takes off from the plateau following the enhanced $D_{\rm cl}$ closely. Evidently, the classical plateau and the threshold ϵ_c shift toward smaller side of ϵ as \hbar decreases. In the plots of D(T) as the function of the scaled parameter ϵ/\hbar^2 shown in Fig. 8(b), the left edges of the plateaus for different \hbar s coincide, which means that $\epsilon_c \propto \hbar^2$. Figure 8(b) also implies that D(T)

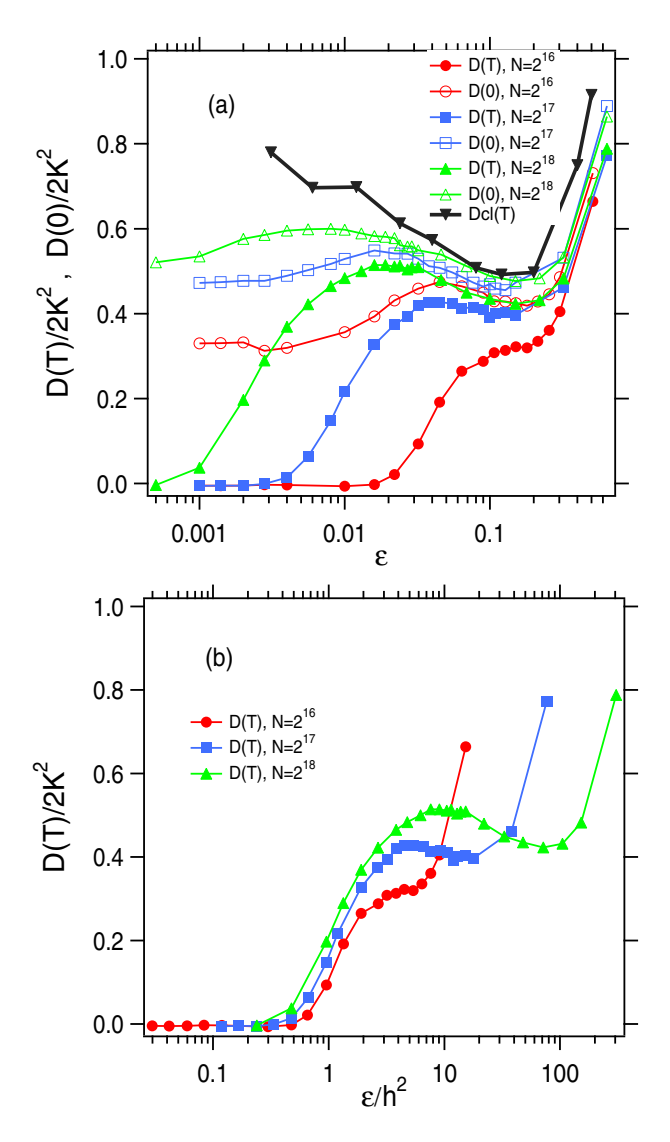


FIG. 8. (a) The time-dependent diffusion coefficient $D(T)/(K^2/2)$ at $T=4\times 10^5$ as a function of ϵ in the monochromatically perturbed SM with $\hbar=\frac{2\pi\,1234}{2^{16}},~\hbar=\frac{2\pi\,1234}{2^{17}},$ $\hbar=\frac{2\pi\,1234}{2^{18}}.$ Here K=3.1 for all data. (b) The D(T) as a function of ϵ/\hbar^2 . Note that the horizontal axes are in logarithmic scale.

is controlled by ϵ/\hbar^2 , as is the case of the localization length of Eq. (9). Thus, the quantum regime we introduced without definition previously should be

$$\epsilon < \epsilon_c (=C \times \hbar^2),$$
 (50)

where the constant C depends on K such as $C \propto K^2$, but we have not confirmed it yet. The localization characteristics of the SM discussed in the previous sections have been confirmed only in the quantum regime. It is still open to question whether or not the localization characteristics represented by Eq. (9) is valid in the semiclassical regime.

The dynamical problems related to the localization process such as the existence of characteristic time leading to the localization and/or the existence of dynamical scaling property are still an interesting unclarified issue, particularly when the LL is extremely large for $\epsilon W\gg 1$ in AM with $W>W^*$ and for $\hbar\to 0$ in SM, respectively.

VII. CONCLUDING REMARKS

We investigated the dynamical localization of the SM and the AM, which are dynamically perturbed by a monochromatically periodic oscillation, and the parameter dependence of the dynamical localization length has been clarified by extensive numerical simulation and theoretical considerations. Under the suitable conditions such systems could be identified with a 2DDS (two-dimensional disordered system) by using the so-called Maryland transform.

The dynamical localization length (LL) was determined by the MSD computed by the numerical wave-packet propagation. We emphasize that the SM is treated in the quantum regime, where the perturbation strength ϵ is smaller than a characteristic value proportional to \hbar^2 . The LL increases exponentially with respect to ϵ in both perturbed SM and AM. It was further scaled by using the dynamical localization length of the unperturbed system in the case of SM, which is consistent with experimental results. On the other hand, in the case of AM, it was scaled by the disorder strength W. There exists the threshold of the disorder strength W^* at which a marked change of W dependence of the dynamical localization length occurs. In the region, $W < W^*$, the ordinary localization in 1DDS occurs, whereas new region, $W > W^*$, peculiar to the quantum map emerged, where the localization length increases with the disorder strength W due to the kicked perturbation.

Next, we showed that all the numerically observed scaling characteristics mentioned above can be reproduced in a *unified manner* by the self-consistent mean-field approximation theory developed for the localization of the 2DDS by introducing a new fundamental characteristic length for the cutoff length. This fact strongly suggests that the monochromatically perturbed SM and AM have essentially the same physical origin for the exponentially enhanced localization length.

Finally the transient diffusive behavior toward the dynamical localization was investigated in the large limit of localization length. In both cases of SM and AM, the transient diffusion coefficient also follows the same scaling rule as the localization rule, but in the case of SM the "classical plateau" exists in the semiclassical regime, in which the compatibility of the quantum localization with the classical chaotic diffusion is quite interesting. Indeed, different type of localization which can not be captured by the above mentioned "unified picture" may emerges in the semiclassical regime. These are interesting problems still open to question.

The Anderson map asymptotically approach to the original Anderson model in the limit of $\tau \to 0$ as mentioned in Sec. II. Whether or not the result in this paper is true even in the time-continuous version (Anderson model) is also an interesting future problem.

ACKNOWLEDGMENTS

This work is partly supported by Japanese people's tax via Grant No. JPSJ KAKENHI 15H03701, and the authors acknowledge them. They are also very grateful to Dr. T. Tsuji and Koike memorial house for use of the facilities during this study.

APPENDIX A: DETERMINATION OF THE COEFFICIENTS A AND D OF EQ. (8)

In this appendix, the details of the \hbar dependence and K dependence of the coefficients A and D in Eq. (8) are given.

First, we show the variation of the coefficient A and coefficient D for the change of K with fixing the ratio $K/\hbar \equiv \kappa$. It is shown in Fig. 9(a) for the three values $\kappa = \kappa_0, \kappa_0/2, \kappa_0/4$, where $\kappa_0 = 18$. Obviously, it turns out that the variation in the value of the coefficient A maintains a nearly constant value when the ratio κ is constant if some irregular variations are ignored. These facts means that A and D, which is a function of κ and K, should be a function of κ only. Next, we change \hbar for various fixed values of K, which is shown in Fig. 10(a). Apparently, for all values of K the dependence $A \propto \hbar^{-2}$ is observed. Since A depends only on κ , the following relation should hold:

$$A = \text{const.} \left(\frac{K}{\hbar}\right)^2 \propto \kappa^2. \tag{A1}$$

Actually, the prediction is confirmed by the fact that the scaled coefficient A/κ^2 is almost constant for different K and κ (and so K and \hbar) as is shown in Fig. 9(c).

On the other hand, the (K/\hbar) dependence of another coefficient D is shown in Figs. 9(b) and 10(b). It is expected that the coefficients D and A should show a similar behavior except for numerical prefactors, i.e., $D \sim A$. However, the K dependence of the coefficient D is less definite and it is often

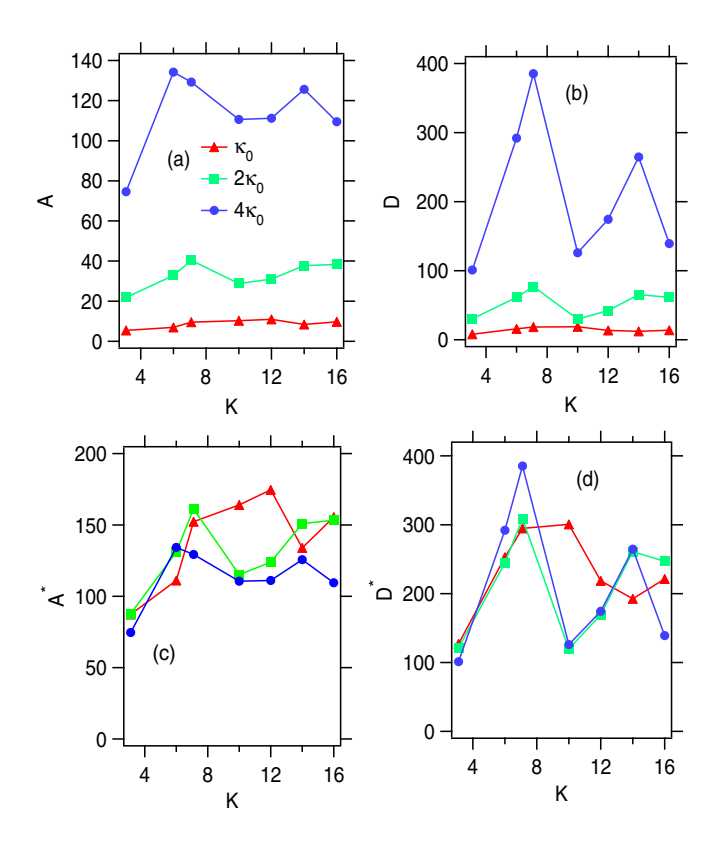


FIG. 9. K dependence of the coefficients (a) A and (b) D of SM with a fixed $\kappa (\equiv K/\hbar)$. The three cases for $\kappa = \kappa_0$, $2\kappa_0$, $4\kappa_0$ ($\kappa_0 = 18$) are shown from below. The scaled coefficients $A^* = A/(\kappa^2/\kappa_{\rm max})$ and $D^* = D/(\kappa^2/\kappa_{\rm max})$, where $\kappa_{\rm max} = 4\kappa_0$, are shown for $\kappa = \kappa_0$, $2\kappa_0$ and $4\kappa_0$ in (c) and (d) of the lower panels, respectively. The three curves almost overlap.

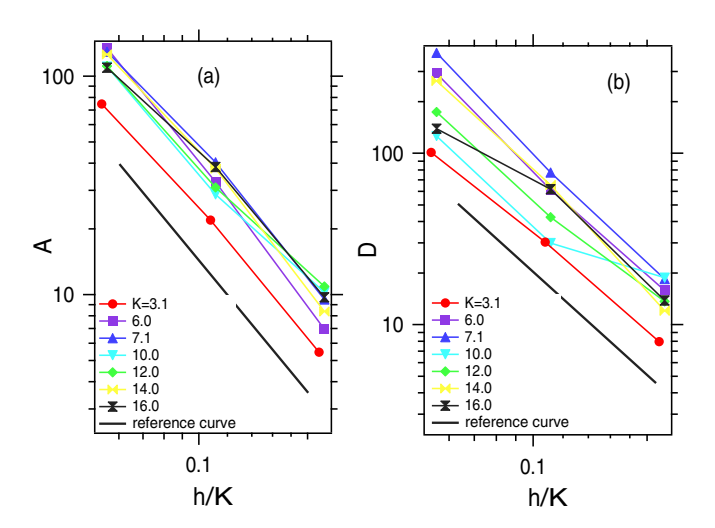


FIG. 10. (a) (\hbar/K) dependence of the coefficients (a) A and (b) D for some K's. Three cases of $\kappa = \kappa_0$, $2\kappa_0$, $4\kappa_0$ ($\kappa_0 = 18$) are shown in the straight lines. Note that the axes are in logarithmic scale. The heavy line shows a straight line with slope of -2 corresponding to the $(\hbar/K)^{-2}$.

accompanied by some irregular fluctuation. This fluctuation becomes more pronounced as the κ is larger, in other words, the smaller \hbar enhances fluctuation, as recognized from Fig. 10(b). This phenomenon is caused by the so-called acceleration modes which are peculiar to the classical dynamics of SM. Actually, in the values of $K = 2n\pi$, where the classical acceleration mode exists, the classical diffusion coefficient $D_{\rm cl}$ increases explosively, and also reflects the localization length of the quantum system as shown in the peak around K = 7. Increasing the perturbation strength ϵ reduces the effect of the acceleration modes. The acceleration modes existing with zero measure in the classical system plays very complicated roles, but it is not essential to the discussion of the quantum localization phenomenon, so we will not discuss it in detail in this paper. If we ignore the fluctuation, the dependence of the coefficient D on K and \hbar in Figs. 9(b) and 10(b) exhibits very similar behavior to the coefficient A, and we conclude that

$$D = \text{const.} \left(\frac{K}{\hbar}\right)^2 \propto \kappa^2. \tag{A2}$$

This prediction is confirmed also by the plot of the scaled coefficient D/κ^2 in Fig. 9(d) in a way parallel to Fig. 9(c).

APPENDIX B: OTHER NUMERICAL DATA THE PERTURBED AM

Figure 11 displays the localization length as a function of scaled perturbation strength ϵW in the monochromatically perturbed AM with the frequencies $\omega_1^{(2)} = \sqrt{2} - 1$, $\omega_1^{(3)} = 1 + 1/\sqrt{17}$ different from one in the text. At least the scaling of the localization length is a stable result even for the frequencies. It follows that for $W > W^*$ the scaled ϵ dependence is overlapping with each other. Also, although not shown here, for $W < W^*$ the W dependence of the localization length in the cases also behaves similarly to that in the text.

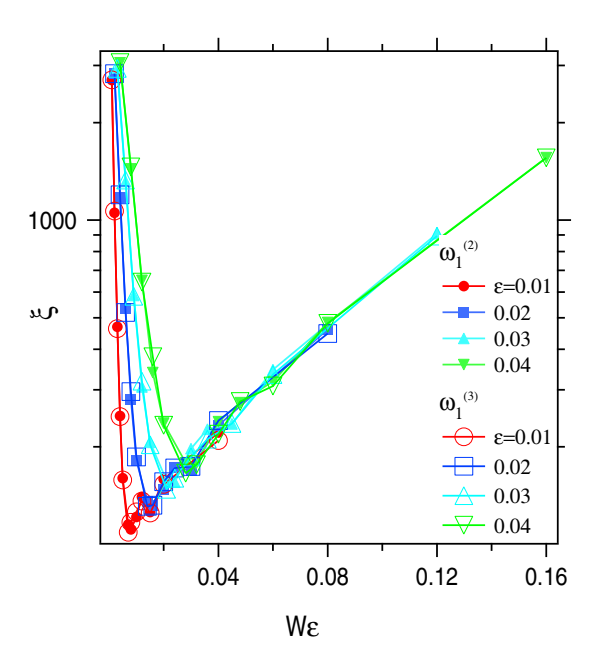


FIG. 11. The localization length as a function of scaled perturbation strength ϵW in the monochromatically perturbed AM for $\epsilon = 0.01, 0.02, 0.03, 0.04$ with perturbation frequencies $\omega_1^{(2)} = \sqrt{2} - 1$, $\omega_1^{(3)} = 1 + 1/\sqrt{17}$. All are displayed together.

APPENDIX C: AUTONOMOUS REPRESENTATION AND MARYLAND TRANSFORM

The eigenvalue problem Eq. (19) can be mapped into the tight-binding form by Maryland transform through the following states $|u_2\rangle$, $|u_1\rangle$ and Hermite matrices \hat{i} , \hat{w} :

$$|u_2\rangle = e^{-i\hat{B}} e^{-i\hat{C}} |u_1\rangle. \tag{C1}$$

$$|u_1\rangle = e^{-i(\hat{A}-\gamma)}|u_2\rangle,$$
 (C2)

$$\frac{1-i\hat{t}}{1+i\hat{t}} = e^{-i\hat{B}}e^{-i\hat{C}},\tag{C3}$$

$$\frac{1 - i\hat{w}}{1 + i\hat{w}} = e^{-i(\hat{A} - \gamma)}.$$
 (C4)

That is,

$$\hat{t}(\hat{q}, \hat{p}, \phi) = -i \frac{1 - e^{-i\hat{B}} e^{-i\hat{C}}}{1 + e^{-i\hat{B}} e^{-i\hat{C}}},$$
(C5)

$$\hat{w}(\hat{p}, \hat{J}) = -i \frac{1 - e^{-i(\hat{A} - \gamma)}}{1 + e^{-i(\hat{A} - \gamma)}} = \tan \left[\frac{(\hat{A} - \gamma)}{2} \right]. \quad (C6)$$

Then the tight-binding form of the eigenvalue problem becomes

$$\left(\tan\left[\frac{(\hat{A}-\gamma)}{2}\right] + \hat{t}(\hat{q},\phi)\right)|\overline{u}\rangle = 0, \tag{C7}$$

where

$$(1+i\hat{t})^{-1}|u_1\rangle = (1-i\hat{t})^{-1}|u_2\rangle$$

$$= (1-i\hat{t})^{-1}e^{i(\hat{A}-\gamma)}|u_1\rangle$$

$$\equiv |\overline{u}\rangle, \qquad (C8)$$

and

$$|\overline{u}\rangle = (|u_1\rangle + |u_2\rangle)/2.$$
 (C9)

 $\hat{t} = \tan[\hat{C}/2]$ when $\epsilon = 0$. We can select a convenient representation for the eigenvalue Eq. (C7). In this case, we dealt with the monochromatic perturbation in the autonomous representation, but the extension to the case of multicolor perturbation can be easily done.

For the SM, the eigenvalue equation in the representation by $u(m,j) = \langle m,j|\overline{u}\rangle$ based on the eigenstates $|m,j\rangle = |m\rangle \otimes |j\rangle$ of \hat{p} and \hat{J} , respectively, is given by the following two-dimensional lattice system with aperiodic and singular on-site potential:

$$\tan\left[\frac{\hbar^2 m^2/2 + j\omega_1 \hbar}{2\hbar}\tau - \frac{\gamma}{2}\right] u(m, j)$$

$$+ \sum_{m', j'} \langle m, j | \hat{t} | m', j' \rangle u(m', j') = 0, \qquad (C10)$$

where the transfer matrix element is given by Eq. (21) in the main text.

On the other hand, for the monochromatically perturbed AM, using

$$\hat{A} = (Wv(\hat{q}) + \omega_1 \hat{J})\tau/\hbar, \tag{C11}$$

$$\hat{B} = \epsilon W v(\hat{q})(\cos \phi) \tau / \hbar, \tag{C12}$$

$$\hat{C} = 2\cos(\hat{p}/\hbar)/\hbar, \tag{C13}$$

the eigenvalue Eq. (C7) is established as it is, then

$$\left(\tan\left[\frac{(\hat{W}(\hat{q}) + \omega_1 \hat{J} - \gamma)\tau}{2}\right] + \hat{t}(\hat{p}, \hat{q}, \phi)\right) |\overline{u}\rangle = 0.$$
(C14)

If we use the representation $u(n,j) (= (\langle n | \otimes \langle j |) | \overline{u} \rangle)$ based on the eigenstates $|q = n\rangle$ of the site \hat{n} and $|j\rangle$ of the \hat{J} , it becomes

$$\tan\left[\frac{Wv_n + j\omega_1\hbar}{2\hbar}\tau - \frac{\gamma}{2}\right]u(n,j) + \sum_{n',j'}\langle n,j|\hat{t}|n',j'\rangle u(n',j') = 0,$$
 (C15)

where

$$\begin{split} \langle n,j|\hat{t}|n',j'\rangle &= \langle n,j|i\frac{e^{-i\hat{B}}-e^{i\hat{C}}}{e^{-i\hat{B}}+e^{i\hat{C}}}|n',j'\rangle \\ &= \langle n,j|i\frac{e^{-i\epsilon Wv(\hat{q})\cos\phi\tau/\hbar}-e^{i2\cos(\hat{p}/\hbar)\tau/\hbar}}{e^{-i\epsilon Wv(\hat{q})\cos\phi\tau/\hbar}+e^{i2\cos(\hat{p}/\hbar)\tau/\hbar}}|n',j'\rangle. \end{split}$$
(C16)

This is the Maryland transformed eigenvalue equation including degrees of freedom of the monochromatic perturbation in the case of the AM.

- [1] K. Ishii, Prog. Theor. Phys. Suppl. **53**, 77 (1973).
- [2] L. M. Lifshiz, S. A. Gredeskul, and L. A. Pastur, *Introduction to the Theory of Disordered Systems* (Wiley, New York, 1988).
- [3] G. Casati, B. V. Chirikov, F. M. Izraelev, and J. Ford, *Stochastic Behavior of a Quantum Pendulum under a Periodic Perturbation*, edited by G. Casati and J. Ford (Springer-Verlag, Berlin, 1979), p. 334.
- [4] G. Casati, I. Guarneri, and D. L. Shepelyansky, Phys. Rev. Lett. 62, 345 (1989).
- [5] F. Borgonovi and D. L. Shepelyansky, Physica D 109, 24 (1997).
- [6] J. Chabé, G. Lemarié, B. Grémaud, D. Delande, P. Szriftgiser, and J. C. Garreau, Phys. Rev. Lett. 101, 255702 (2008).
- [7] J. Wang and A. M. Garcia-Garcia, Phys. Rev. E 79, 036206 (2009).
- [8] G. Lemarie, H. Lignier, D. Delande, P. Szriftgiser, and J.-C. Garreau, Phys. Rev. Lett. 105, 090601 (2010).
- [9] C. Tian, A. Altland, and M. Garst, Phys. Rev. Lett. 107, 074101 (2011).
- [10] M. Lopez, J. F. Clement, P. Szriftgiser, J. C. Garreau, and D. Delande, Phys. Rev. Lett. 108, 095701 (2012).
- [11] M. Lopez, J.-F. Clement, G. Lemarie, D. Delande, P. Szriftgiser, and J. C. Garreau, New J. Phys. 15, 065013 (2013).
- [12] H. S. Yamada, F. Matsui, and K. S. Ikeda, Phys. Rev. E 92, 062908 (2015); H. S. Yamada and K. S. Ikeda (unpublished).
- [13] D. L. Shepelyansky, Physica D 8, 208 (1983).
- [14] S. Fishman, D. R. Grempel, and R. E. Prange, Phys. Rev. Lett. 49, 509 (1982); D. R. Grempel, R. E. Prange, and S. Fishman, Phys. Rev. A 29, 1639 (1984); R. E. Prange, D. R. Grempel, and S. Fishman, Phys. Rev. B 29, 6500 (1984).

- [15] I. Manai, J.-F. Clement, R. Chicireanu, C. Hainaut, J. C. Garreau, P. Szriftgiser, and D. Delande, Phys. Rev. Lett. 115, 240603 (2015).
- [16] E. Doron and S. Fishman, Phys. Rev. Lett. **60**, 867 (1988).
- [17] B. Toloui and L. E. Ballentine, Quantum Localization for Two Coupled Kicked Rotors, arXiv:0903.4632.
- [18] H. Yamada and K. S. Ikeda, Phys. Lett. A 328, 170 (2004).
- [19] H. S. Yamada and K. S. Ikeda, Eur. Phys. J. B 87, 208 (2014).
- [20] H. S. Yamada and K. S. Ikeda, Phys. Rev. E **82**, 060102(R) (2010); Eur. Phys. J. B **85**, 41 (2012); **85**, 195 (2012).
- [21] D. Vollhardt and P. Wölfle, Phys. Rev. Lett. 45, 842 (1980);Phys. Rev. B 22, 4666 (1980); Phys. Rev. Lett. 48, 699 (1982).
- [22] P. Wolfle and D. Vollhardt, Int. J. Mod. Phys. B **24**, 1526 (2010).
- [23] The average over irrational random number is more efficient than the normal random number average, because $U(s,\phi_0)$ is a periodic with respect to ϕ_0 .
- [24] Numerically, we confirmed that the average over ϕ_0 does not change very significantly the result averaged over n_0 .
- [25] M. Kappus and F. Wegner, Z. Phys. B 45, 15 (1981).
- [26] B. Derrida and E. J. Gardner, J. Phys. 45, 1283 (1984).
- [27] J. L. Pichard, J. Phys. C 19, 1519 (1986).
- [28] J. Kroha, Physica A 167, 231 (1990).
- [29] S. Adachi, M. Toda, and K. Ikeda, Phys. Rev. Lett. 61, 659 (1988); B. Gadway, J. Reeves, L. Krinner, and D. Schneble, *ibid.* 110, 190401 (2013).